

## Roughness of Face-Milled Surface Topography in Directions Relative to the Feed Movement

Antal Nagy (0000-0001-6160-4973), János Kundrák (0000-0002-6013-7856)

Institute of Manufacturing Science, Faculty of Mechanical Engineering and Informatics, University of Miskolc, H-3515 Miskolc, Hungary. E-mail: [antal.nagy@uni-miskolc.hu](mailto:antal.nagy@uni-miskolc.hu), [janos.kundrak@uni-miskolc.hu](mailto:janos.kundrak@uni-miskolc.hu)

By achieving the accuracy and roughness requirements imposed on the connecting surfaces of machine components –the topography created during machining – it is guaranteed to meet the operational requirements. We cannot ignore the fact that if connected milled plane surfaces move in different directions relative to each other during operation, there may be different contact conditions caused by the unevenness of the topography. The direction-dependent roughness irregularities and functional characteristics of the topography are not sufficiently explored, thus in this work we examine the roughness and its deviations by assuming displacements in different directions compared to the feed motion during operation. The inhomogeneity of the topography is analyzed with a symmetrical milling setup on a face-milled surface, with profiles measured in plane sections parallel to and in 8 other different directions from the feed. The degree and distribution of deviations of the recorded roughness profiles, the selected amplitude and functional roughness values are examined at several points of the measurement planes.

**Keywords:** Face milling, Surface roughness, Distribution of roughness

### 1 Introduction

By properly manufacturing machine parts, the expected quality of operation is ensured during their planned service life. For connecting surfaces, various functional properties can be prescribed, in the case of fixed or relatively moving pairs of surfaces during operation [1].

The service life of the part is strongly influenced by the quality of the machined surfaces (surface layer

state and topography) [2]. A great number of parameters are available for characterizing roughness to suit different requirements [3]. Roughness profile parameters are presented in Fig. 1, classified into 4 groups: amplitude, spacing, hybrid and functional types [4]. We examine the values of  $R_a$ ,  $R_z$  and  $R_{sk}$ ,  $R_{ku}$  among the amplitude parameters, and  $R_k$ ,  $R_{pk}$  and  $R_{vk}$  among the functional parameters.

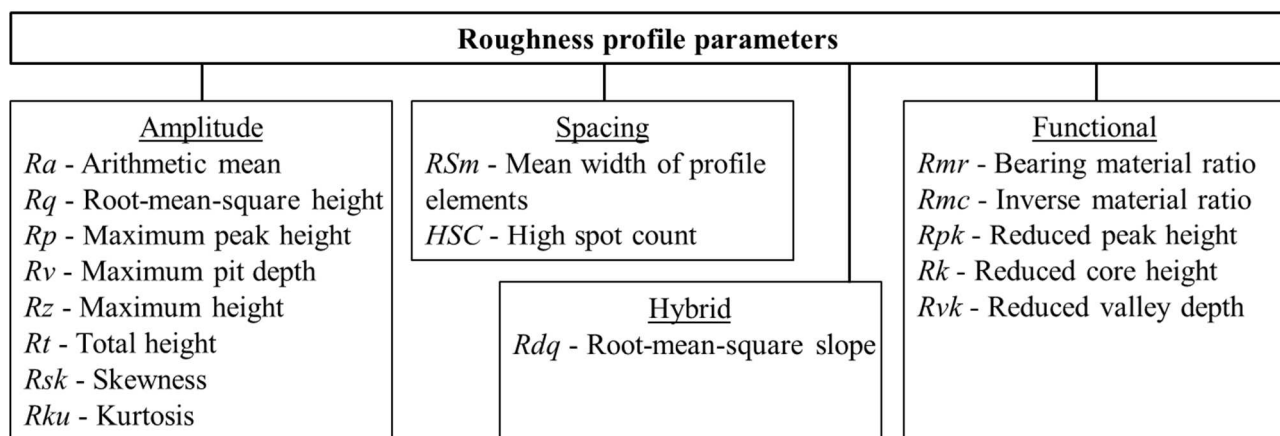


**Fig. 1** Classification of 2D roughness parameters [5]

The amplitude parameters describe the height characteristics of the profiles measured on the surface. They show the smoothness of the surface microgeometry, the load capacity, the height of the peaks and valleys, the density, the spikiness and the symmetry to the center line [4,5], but they do not give

information about the width and slope of the irregularities. The parameters can be used to characterize the lubricant retaining ability [6], the wear resistance [7] of the surface, the degree of the wear [8], and the degree of plastic deformation of the peaks during finishing [9].

Among these,  $R_a$  and  $R_z$  are the most frequently used parameters in industry [10]. This has a historical reason; they could be measured with the early analog roughness measurement techniques [11], therefore we have information on a broad range of surfaces with these indices [12]. On one hand, the production processes can be characterized with these roughness parameters [13]. Although, their value changes have no or weak correlation with the functional characteristics of the surfaces [12]. Thus, we can provide more details about the functionality of the surface when considering other parameters as well [14].

One of the frequently studied profile or topography specifications is the amplitude density function and its characteristic skewness ( $R_{sk}$ ) and kurtosis ( $R_{ku}$ ). These statistical parameters are related to the contact area of the surface, friction, wear, and fatigue strength [15].  $R_{sk} < 0$  predicts dense peaks on the topography, thus a larger contact area, larger coefficient of friction and better lubrication conditions [16]. When this is combined with a relatively high value of  $R_{ku} > 3$ , the turned [3], end-milled [17], or plateau honed [18] surface has better load bearing properties and a lower coefficient of friction. On the micromilled topography a place for the lubricant or chip is formed, which is indicated by the measured  $R_{sk} \approx 0$ , and due to the sharp peaks of the milling marks, the running-in time is short if the surface slides, where  $R_{ku} > 3$  [19]. The tool edge geometry has a significant effect on the values of these parameters, since the shape of the cutting marks affects the texture of the topography, thus its amplitude density function [3].

The functional characteristics of surfaces are often analyzed with the Abbott-Firestone (amplitude distribution) curve (AFC) and the parameters derived from it [20]. The degree of corrosion resistance can be determined from the shape of the curve [21]. For further functional analysis, the height of the three zones (peak, core and valley) of the curve is characterized by the parameters  $R_{pk}$ ,  $R_k$ , and  $R_{vk}$  [20].  $R_{pk}$  shows the height of the outstanding material part that wears off first during sliding [22]. Its value refers to the height and sharpness of the peaks [19] and the size of the specific contact area, thus the surface pressure [22] and the contact stress [23]. In the case of a moving surface, it is related to the duration of the running-in period [24]. A small value of the parameter shows better wear resistance [25] and shorter wear time [24].  $R_k$  expresses the layer thickness available on the contact surface for the stable wear (before critical wear period) [19,24]. A small value measured on a surface indicates better surface load capacity, greater stress resistance [25], and improved sliding conditions between contacting surfaces [23]. A decreased  $R_k$  value is expected in machining with a defined edge

tool when the cutting speed is increased, or the feed value is reduced [26].  $R_{vk}$  shows the depth of the non-contact valley part, a measure of the topography's ability to retain lubricant [24,25]. A higher value is advantageous for feeding, circulating and storing the oil during operation [27].

Little attention is given to roughness-based functional studies of face-milled surfaces compared to other processes. So far, it has been found that sharp peaks and valleys are usually formed on the topography, where a relatively small friction coefficient is expected in case of sliding ( $R_{ku} \approx 3-4$ ) [28], but sometimes the topography's peaks and valleys are rounded ( $R_{ku} \approx 2$ ) [17]. Furthermore, small positive ( $\approx 0.2$ ) (where the profiles have a nearly normal distribution) or negative  $R_{sk} \approx -0.1$  to  $-0.7$  values (in this case the peaks are denser than the valleys) can often be measured on surfaces, with negative values providing more favorable wear resistance and load-bearing capacity of the surface [28]. The evolution of the values is significantly influenced by the edge geometry of the tool, the material of the tool and workpiece, as well as the applied cutting data [17,28]. In general, face-milled surfaces have poor running-in and stable wear properties and poor lubrication characteristics, where  $R_{pk}$  and  $R_k$  values are relatively high compared to  $R_{vk}$  [29]. The Abbott-Firestone curve of the topography is typically linear, so it has good corrosion resistance, but the possibility of stress corrosion on sharp ridges must be considered [21].

As a result of the face milling motion conditions (tool rotation and workpiece linear movement), a complex topography is produced on the machined surface. As illustrated in Fig. 2, the profiles measured in the feed direction are periodic, but they have varying heights according to their position from the plane of symmetry (traverse path of the tool axis). The characteristics of the profiles differ greatly when measured in perpendicular direction [30]. This variation affects the functional properties of the surface in its different parts.

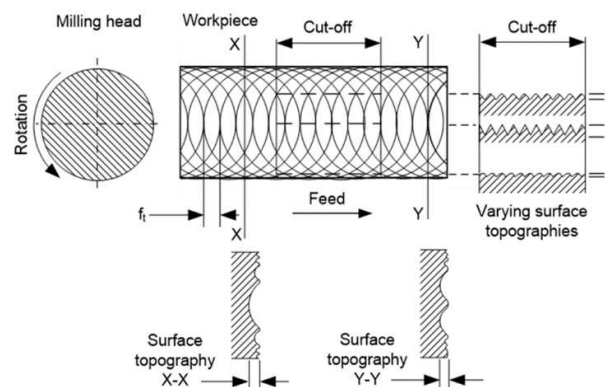


**Fig. 2** Change in profile characteristics measured in different directions on face-milled surface [30]

Based on the literature reviewed above, we conclude that, although there is research on the determination of functional characteristics and the exploration of their correlations with topographical parameters, these studies either do not or only rarely consider sliding surfaces that move in different directions during operation. In this article, our aim is to contribute to the exploration of this scientific research gap. For this, we examine the face-milled surface topography in a new approach; its direction-dependent roughness and deviations are analyzed with several roughness parameters simultaneously.

## 2 Experimental conditions

For this study, we measured the roughness of a milled surface and selected the roughness parameters.

### 2.1 Experimental settings

The face milling experiment was carried out on a PerfectJet MCV-M8 vertical CNC machining machine. The plane surface on a normalized C45 material grade workpiece with an area of  $58 \times 50 \text{ mm}^2$  was machined with a single ATORN OCKX 0606-AD-TR, HC4640 grade insert ( $\gamma_r = 43^\circ$ ;  $\gamma_o = 25^\circ$ ;  $\alpha_o = 7^\circ$ ;  $r_s = 0.5 \text{ mm}$ ) in an ATORN 10612120 face milling head (nominal diameter:  $D_t = 80 \text{ mm}$ ). The set cutting speed was  $v_c = 300 \text{ m/min}$ , the feed per tooth was  $f_z = 0.4 \text{ mm/tooth}$  and the cutting depth was  $a_p = 0.4 \text{ mm}$ . The topography was created by face milling with a symmetrical setting, i.e. the tool axis moved above the center line of the machined surface. The tool edge only chipped the surface during its front-cutting movement, thus forming single cutting marks on it. In doing so, the range of the feed movement of the workpiece lasted from the first contact of the tool edge until the center of the tool.

### 2.2 Roughness analysis, method and parameters

After machining, we measured the profile roughness of the milled surface with a CL2 confocal chromatic sensor on an AltiSurf 520 topography measuring device. To examine the roughness deviations, several measurement points were defined on the surface in the symmetry plane and on three squares with the same center. These mark the centers of the measured profiles and align to measurement planes which form different angles to the feed (Fig. 3). The symmetry plane ( $\Delta$ ) and the measurement planes rotated incrementally by  $15^\circ$  from it are marked with large Greek letters; thus  $\Delta - 0^\circ$ ,  $\text{B} - 15^\circ$ ,  $\text{I} - 30^\circ$ ,  $\Delta - 45^\circ$ ,  $\text{E} - 60^\circ$ ,  $\text{Z} - 75^\circ$ ,  $\text{H} - 90^\circ$ . The order of the points along these planes follows the path of the tool edge in the workpiece material. The planes marked with a small Greek letter are reflected on the middle plane, so their angle and the order of the points on those planes are symmetric to their counterpart –

in this case  $\text{I}$  and  $\text{Y}$  (with an angle of  $-30^\circ$ ) and  $\text{E}$  and  $\text{e}$  (with an angle of  $-60^\circ$ ) form pairs. The directions of the examination planes (marked with arrows in Fig. 3) show the direction of the roughness measurement. During the analysis of all profiles, an evaluation length of  $4 \text{ mm}$  and a section length of  $0.8 \text{ mm}$  specified in ISO 21920:2021 standard were set. The measurement results were evaluated with the AltiMap Premium software.

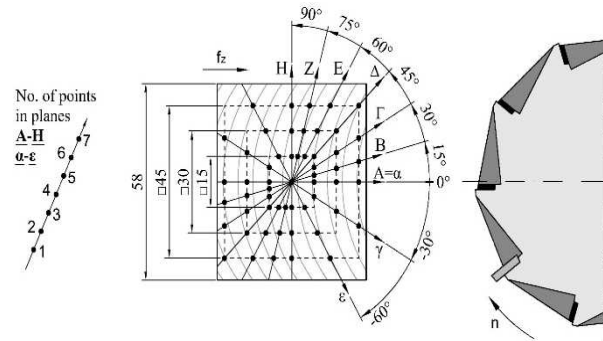


Fig. 3 Positions of the measurement planes and points

$$Ra = \frac{1}{l_n} \int_0^{l_n} |z(x)| dx \quad (1)$$

$$Rz = \frac{1}{n} \left( \sum_{i=1}^n Rp_i - \sum_{i=1}^n Rv_i \right) \quad (2)$$

Where:

$l_n$ ...Evaluation length [mm],

$z(x)$ ...Height of one surface point [ $\mu\text{m}$ ],

$n$ ...Number of sections [-],

$Rp_i$ ...Highest peak height within a section length [ $\mu\text{m}$ ],

$Rv_i$ ...Lowest valley depth within a section length [ $\mu\text{m}$ ].

During the test, we analyze the amplitude  $Ra$ ,  $Rz$  and  $Rsk$ ,  $Rku$ , as well as the functional parameters  $Rk$ ,  $Rpk$  and  $Rvk$ . The average roughness ( $Ra$ ) is the average absolute deviation of the roughness irregularities from the mean line (1), the maximum height ( $Rz$ ) is the difference in height between the average of the five highest peaks and the five lowest valleys (2) [4].

The  $Rsk$  skewness (3) and  $Rku$  kurtosis (4) parameters are calculated from the amplitude density function of the roughness profiles. For a Gaussian surface, the distribution of peaks and valleys is symmetrical to the center line ( $Rsk = 0$ ) [4] and  $Rku = 3$  [3]. A profile with narrow, deep scratch marks and wide peaks has a value of  $Rsk < 0$ , or vice versa, in which case  $Rsk > 0$  [26]. The value of  $Rku$  is related to the spikiness and width of the peaks and valleys [4]. Fig. 4 illustrates this.

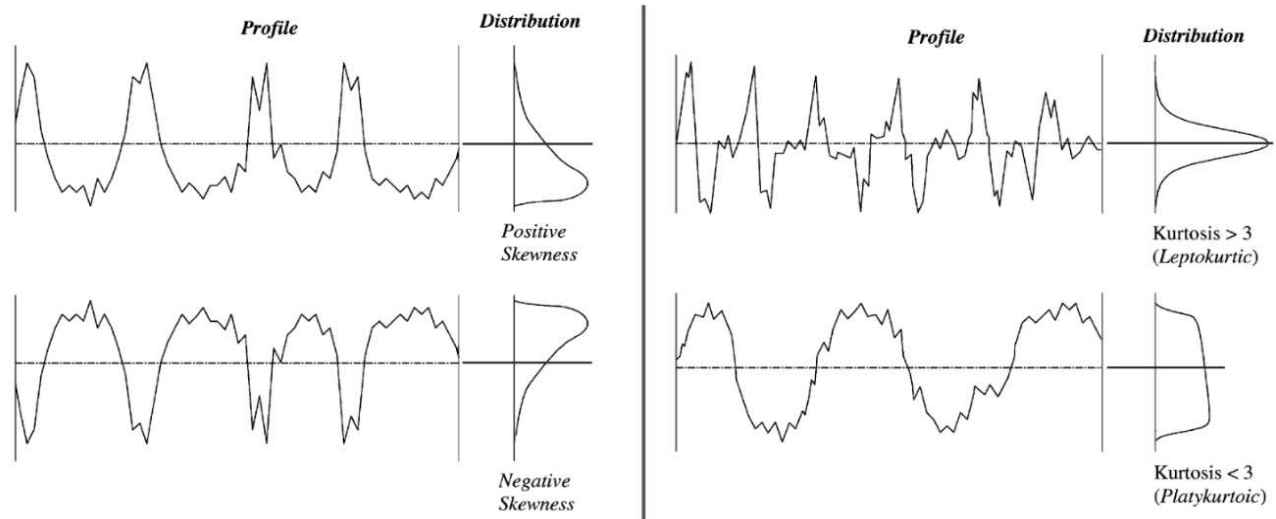


**Fig. 4** Different types of density function curves with the values of  $Rsk$  and  $Rku$  [4]

$$Rsk = \frac{1}{Rq^3} \int_{-\infty}^{\infty} z^3(x) dx \quad (3)$$

$$Rku = \frac{1}{Rq^4} \int_{-\infty}^{\infty} z^4(x) dx \quad (4)$$

Where:

$Rq$ ...Root mean square height parameter [ $\mu\text{m}$ ].

$Rpk$ ,  $Rk$ , and  $Rvk$  are the parameters describing the height of the peak, core, and valley zones of the

Abbott-Firestone curve of the roughness profile (Fig. 5). To determine these, the curve is first divided into three parts with an equivalent straight line covering a 40% material proportion, which intersects the  $Mr = 0\%$  and  $Mr = 100\%$  abscissae. The height difference between the two points is  $Rk$  reduced core height. Above and below the intersection points, the areas under the curve are simplified into right-angled triangles, the height of whose sides are  $Rpk$  reduced peak height and  $Rvk$  reduced valley depth [13].

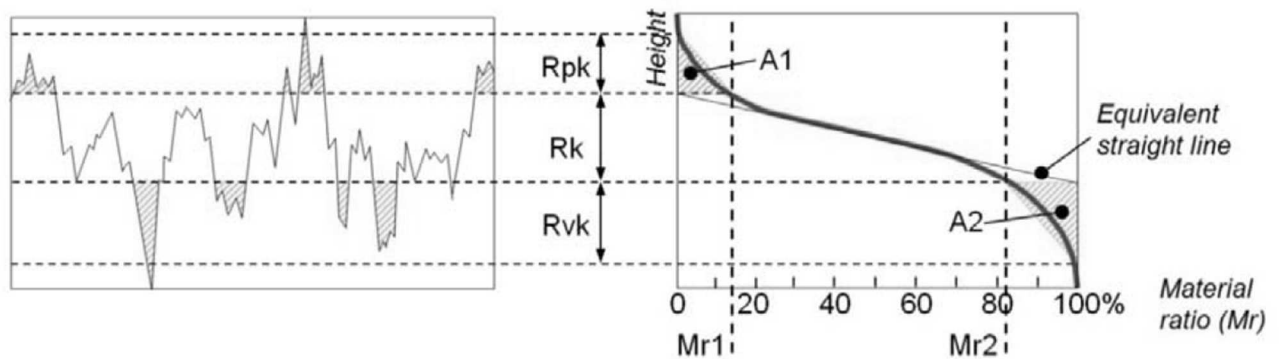


**Fig. 5** Abbott-Firestone curve of the profile and the height parameters of the three zones [31]

### 3 Results and Discussion

After performing the face milling experiments and roughness measurements, the effect of the measurement direction on the roughness, deviations, and functional characteristics of the face-milled surface is analyzed. For this purpose, we evaluate the roughness curves and parameter values of the profiles measured in the planes and analyze their deviations and distributions. We report the values of the selected amplitude  $Ra$ ,  $Rz$ ,  $Rsk$  and  $Rku$  and the functional  $Rpk$ ,  $Rk$ , and  $Rvk$  parameters of the profiles measured at the points in each plane (in a given direction angle) in Tables 1–7. We also give the arithmetic mean of the

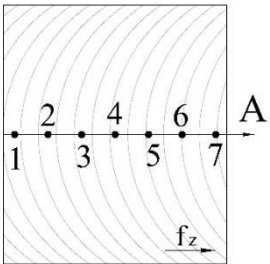
values measured in the plane ( $\bar{R}$ ), the size of the deviations ( $\Delta R$ ), and their ratio ( $\Delta R/\bar{R}$ ). Since the  $Rsk$  parameter can have a positive or negative value according to its definition, its  $\Delta R/\bar{R}$  quotient is not a representative indicator of plane deviations, so this value is not given in the tables. Among the profiles measured on the topography, the roughness profile curves measured at points 2, 4, and 6 of the test planes B, E, and H are shown in Fig. 6.

#### 3.1 Analysis of roughness in the measurement planes

In the discussion, we first analyze the results obtained in the measurement planes.

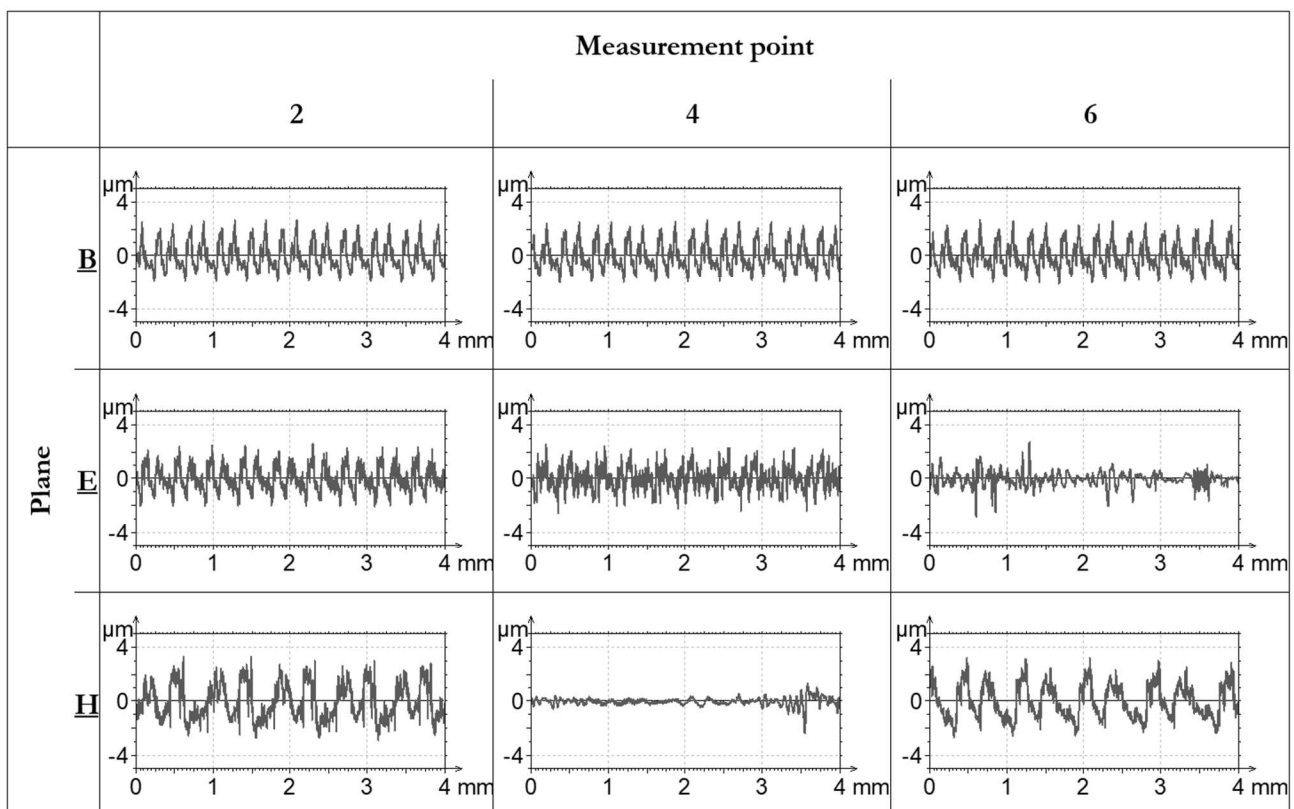
**Tab. 1** Roughness values in plane  $\underline{A} - 0^\circ$ 

Point no.	1	2	3	4	5	6	7	$\bar{R}$	$\Delta R$	$\Delta R/\bar{R}$
$Ra$ [ $\mu m$ ]	1.44	1.43	1.45	1.46	1.43	1.43	1.45	1.44	0.02	1.6%
$Rz$ [ $\mu m$ ]	7.13	6.95	7.10	7.00	6.96	7.01	7.03	7.03	0.17	2.4%
$Rsk$ [-]	0.17	0.13	0.15	0.14	0.17	0.16	0.12	0.15	0.06	
$Rku$ [-]	2.18	2.11	2.16	2.12	2.15	2.15	2.11	2.14	0.07	3.2%
$Rpk$ [ $\mu m$ ]	1.56	1.31	1.53	1.44	1.39	1.38	1.35	1.42	0.25	17.6%
$Rk$ [ $\mu m$ ]	5.03	5.13	4.99	5.12	5.04	5.05	5.14	5.07	0.14	2.8%
$Rvk$ [ $\mu m$ ]	0.46	0.45	0.48	0.41	0.41	0.47	0.44	0.45	0.07	16.0%



In the feed directional plane  $\underline{A}$  ( $0^\circ$ ), the value of  $Rsk$  is positive and close to 0 and  $Rku < 3$  at all points (Table 1). These values indicate the nature of the profiles, that the areas of the peaks and valleys are nearly symmetric to the center line and are flatter compared to the profile elements of a Gaussian surface. Based on these – assuming a displacement in the feed direction – the texture is unfavorable from the point of view of friction and load bearing, based on the findings in [17]. The average values of the functional parameters (high  $Rpk$  and  $Rk$ , low  $Rvk$  values) and ratios also indicate the poor wear and lubrication properties of the face-milled surface [29].

The deviation of values of the examined parameters is negligible, typically below 3.5%, and the differences in  $\Delta Rsk = 0.05$ ,  $\Delta Rpk = 0.25 \mu m$  and  $\Delta Rvk = 0.07 \mu m$  are also small. So, in this direction, at any location, the measurement results and functional characteristics are almost identical. While theoretically the same profiles can be measured at the measurement points, the negligible differences experienced on the real surface can be caused by heterogeneity of the workpiece material, plastic deformation, dynamic effects, and other transient phenomena in the cutting process, or the error of the roughness measuring device.

**Fig. 6** Roughness profile curves in planes  $\underline{B}$ ,  $\underline{E}$  and  $\underline{H}$ 

In the  $15^\circ$  plane  $\underline{B}$ , the average values of the parameters are almost identical to the values of plane  $\underline{A}$ ; although their differences have increased, they remain negligible in most cases (Table 2). For most parameters, the differences do not reach 6%, and  $\Delta Rsk = 0.15$  and  $\Delta Rvk = 0.15 \mu m$  are also small. The

reason for the significant (46.2%) deviation of the  $Rpk$  values is probably the slight change in the shape of the Abbott-Firestone curves, which affects the value of  $Rpk$  during evaluation. Namely, the shape and height of the roughness profile curves measured in the plane are almost the same (Fig. 6). The results show that

when the milled surface moves in this direction, the functional characteristics are expected to be almost identical to those described in plane A.

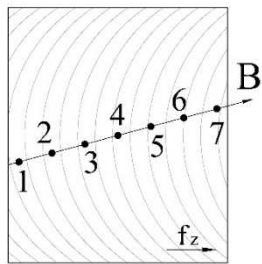
The distribution of the values in the first two analyzed planes is the same for the examined parameters. An exception is the random change in values of  $Rpk$ .

The arithmetic mean values in the  $30^\circ$  I plane are almost identical to the average values measured in planes A and B, except for  $Rpk$ , which shows 20–30% lower values (Table 3). Here, too, the reason for the difference is presumably the minimal change in the shape and the evaluation of the Abbott-Firestone curves. The deviations of the parameter values are

small, a maximum of 10.2%, and the values  $\Delta Rsk = 0.21$ ,  $\Delta Rpk = 0.48 \mu\text{m}$ , and  $\Delta Rvk = 0.12 \mu\text{m}$  are very similar to those calculated in plane B. Hence, the wear and lubrication characteristics at in-plane locations are almost identical. Their distribution is characterized by the fact that the maximum value is at point 4 (in the symmetry plane) and at point 3 for  $Rpk$  and  $Rvk$ , and they decrease in both directions the further away from it. In summary, in the case of an assumed displacement of the topography in this direction, a minimal reduction in running-in period can be expected, as well as very similar wear resistance, load bearing, and lubrication properties, as in the case of displacement in the direction of plane A or B.

**Tab. 2** Roughness values in plane B –  $15^\circ$

Point no.	1	2	3	4	5	6	7	$\bar{R}$	$\Delta R$	$\Delta R/\bar{R}$
$Ra [\mu\text{m}]$	1.42	1.41	1.41	1.40	1.42	1.38	1.40	1.41	0.03	2.3%
$Rz [\mu\text{m}]$	6.80	6.80	6.88	6.90	6.94	6.90	6.68	6.84	0.26	3.7%
$Rsk [-]$	0.07	0.08	0.17	0.10	0.13	0.08	0.02	0.09	0.15	
$Rku [-]$	2.07	2.09	2.15	2.12	2.11	2.12	2.02	2.10	0.13	6.2%
$Rpk [\mu\text{m}]$	1.24	1.31	1.50	1.23	1.24	1.19	0.93	1.23	0.56	45.6%
$Rk [\mu\text{m}]$	4.92	4.86	4.85	4.90	5.02	4.79	4.91	4.89	0.22	4.5%
$Rvk [\mu\text{m}]$	0.53	0.56	0.43	0.53	0.47	0.58	0.57	0.53	0.15	28.4%

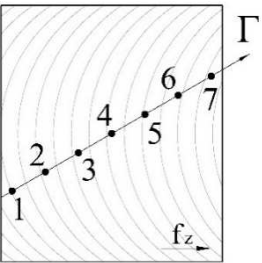


Based on the functional parameter values in the I–I planes it can be stated that the surface has poor wear resistance, dimensional stability [29] and a relatively high coefficient of friction [23], which is indicated by the high  $Rk$  values compared to the values of  $Rpk$  and

$Rvk$ . Also, the relationship  $Rvk < Rpk$  indicates that the valleys of the roughness profiles are shallow, so they probably cannot provide adequate lubrication to the functional surface [27].

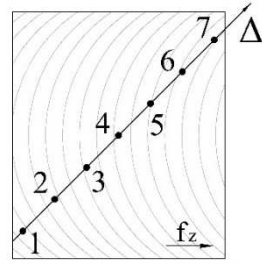
**Tab. 3** Roughness values in plane I –  $30^\circ$

Point no.	1	2	3	4	5	6	7	$\bar{R}$	$\Delta R$	$\Delta R/\bar{R}$
$Ra [\mu\text{m}]$	1.32	1.37	1.40	1.38	1.38	1.33	1.27	1.35	0.14	10.2%
$Rz [\mu\text{m}]$	6.31	6.67	6.85	6.99	6.97	6.79	6.86	6.78	0.68	10.0%
$Rsk [-]$	-0.06	0.04	0.09	0.15	0.13	0.11	0.09	0.08	0.21	
$Rku [-]$	1.93	2.02	2.06	2.14	2.12	2.06	2.08	2.06	0.21	10.0%
$Rpk [\mu\text{m}]$	0.71	1.03	1.19	1.06	1.04	0.93	0.81	0.97	0.48	50.1%
$Rk [\mu\text{m}]$	4.64	4.82	4.91	5.06	5.02	4.90	4.72	4.87	0.42	8.6%
$Rvk [\mu\text{m}]$	0.55	0.53	0.48	0.53	0.59	0.55	0.60	0.55	0.12	21.0%



**Tab. 4** Roughness values in plane A –  $45^\circ$

Point no.	1	2	3	4	5	6	7	$\bar{R}$	$\Delta R$	$\Delta R/\bar{R}$
$Ra [\mu\text{m}]$	1.23	1.27	1.37	1.36	1.28	1.01	0.54	1.15	0.83	72.3%
$Rz [\mu\text{m}]$	6.00	6.01	6.91	6.95	6.94	6.57	4.20	6.23	2.76	44.3%
$Rsk [-]$	0.16	-0.05	0.08	0.17	0.23	0.04	0.13	0.11	0.28	
$Rku [-]$	2.09	1.89	2.07	2.12	2.16	2.56	4.26	2.45	2.37	96.8%
$Rpk [\mu\text{m}]$	0.95	0.43	0.93	0.95	1.13	0.89	0.90	0.88	0.70	79.6%
$Rk [\mu\text{m}]$	4.01	4.62	5.03	5.01	4.35	3.53	1.27	3.97	3.76	94.7%
$Rvk [\mu\text{m}]$	0.58	0.48	0.55	0.57	0.57	0.91	0.93	0.65	0.45	68.5%



In the A plane, the mean values are significantly lower for  $Ra$ ,  $Rz$ ,  $Rpk$ , and  $Rk$  (by up to 38%), higher for  $Rku$  and  $Rvk$  (by up to 47%) compared to plane A, and similar for  $Rsk$  (Table 4). The deviations of the parameter values are high (between 44–97%), so in the case of sliding in this direction, a remarkable change

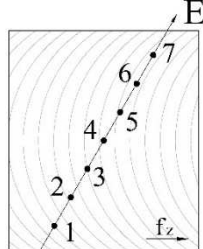
in the functional characteristics can be expected in different parts of the surface. The values of the parameters at points 1–4 show a small (below 25%) difference, then moving away from point 4 to points 5–7 the degree of deviation progressively increases. Exceptions are the values of  $Rsk$ ,  $Rpk$ , and  $Rvk$ , which

are minimal at point 2 and whose deviations are smaller at points 4–7 (below 39%), as well as the random nature of change. In summary, at the measurement locations 1–4, the parameter values

indicate similar topography properties as in planes  $\underline{A}$ – $\underline{C}$ , however, moving away from point 4 towards point 7, the surface becomes smoother and its friction, wear, and lubrication characteristics improve [17,25,27].

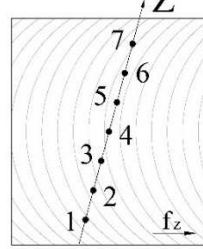
**Tab. 5** Roughness values in plane  $\underline{E}$  – 60°

Point no.	1	2	3	4	5	6	7	$\bar{R}$	$\Delta R$	$\Delta R/\bar{R}$
$Ra$ [ $\mu\text{m}$ ]	1.21	1.27	1.30	1.26	0.98	0.54	0.79	1.05	0.76	72.2%
$Rz$ [ $\mu\text{m}$ ]	6.03	6.32	7.02	6.86	6.77	4.28	6.38	6.24	2.74	43.9%
$Rsk$ [-]	0.10	-0.03	0.18	0.27	0.34	-0.13	0.35	0.15	0.48	
$Rku$ [-]	2.12	1.95	2.19	2.23	2.76	4.47	3.79	2.79	2.52	90.6%
$Rpk$ [ $\mu\text{m}$ ]	0.94	0.51	1.08	1.20	1.13	0.85	1.29	1.00	0.78	77.8%
$Rk$ [ $\mu\text{m}$ ]	3.90	4.68	4.60	4.25	3.19	1.48	2.38	3.50	3.21	91.6%
$Rvk$ [ $\mu\text{m}$ ]	0.66	0.56	0.61	0.65	0.76	0.97	1.04	0.75	0.48	63.7%



**Tab. 6** Roughness values in plane  $\underline{Z}$  – 75°

Point no.	1	2	3	4	5	6	7	$\bar{R}$	$\Delta R$	$\Delta R/\bar{R}$
$Ra$ [ $\mu\text{m}$ ]	1.22	1.22	1.18	0.93	0.48	0.81	1.12	0.99	0.75	75.1%
$Rz$ [ $\mu\text{m}$ ]	6.64	6.81	6.87	6.43	3.84	6.03	7.51	6.30	3.67	58.3%
$Rsk$ [-]	0.13	0.10	0.30	0.14	-0.60	0.13	0.30	0.07	0.90	
$Rku$ [-]	2.18	2.14	2.37	2.78	4.72	3.10	2.66	2.85	2.58	90.6%
$Rpk$ [ $\mu\text{m}$ ]	0.88	0.80	1.24	1.00	1.02	1.12	1.23	1.04	0.44	42.3%
$Rk$ [ $\mu\text{m}$ ]	4.16	4.40	3.85	3.05	1.09	2.62	3.68	3.27	3.31	101.4%
$Rvk$ [ $\mu\text{m}$ ]	0.64	0.66	0.68	0.92	1.28	0.94	0.79	0.84	0.63	75.2%



In planes  $\underline{E}$  (60°, Table 5),  $\underline{Z}$  (75°, Table 6), and  $\underline{H}$  (90°, Table 7) the parameter values change in the same way, so they are analyzed together. The average values compared to the  $\underline{A}$  plane are similar in the  $\underline{E}$  and  $\underline{Z}$  planes and differ by 13–32% in the 90°  $\underline{H}$  plane. The deviation of parameter values is high (38–126.2%), and with the increase of the direction angle they increase in the case of  $Ra$ ,  $Rz$ ,  $Rsk$ , and  $Rk$ , they decrease minimally in the case of  $Rku$  and the values of  $Rpk$  and  $Rvk$  parameters show no correlation. The nature of the change in values – shifted by one measurement point in the following plane – is the same (except for  $Rpk$  and  $Rvk$ ). The reason for this can be explained as follows. Note that a non-feed direction measurement plane intersects different milling marks at different angles (as illustrated in Fig. 4). Where the plane is in a tangential position to

the adjacent cutting mark, a recorded profile lies as a chord on the side of the ridge. Therefore, the roughness profile curve on the plane here is the smoothest, it has the smallest height and the widest profile element (Fig. 6). It follows that the measurement point nearest to this (points  $\underline{E}6$ ,  $\underline{Z}5$  or  $\underline{H}4$ ) has minimum  $Ra$ ,  $Rz$ ,  $Rsk$ ,  $Rk$ , and maximum  $Rku$  values. The reason behind the change in the location of the extreme values is that the different planes are tangential to the milling marks at different places, at different distances from the plane of symmetry. In summary – for all three planes – the best wear resistance, sliding, and lubrication characteristics are expected in the measurement point with the extreme values in the given direction, and these properties are expected to deteriorate further away from this location in two directions [17,25,27].

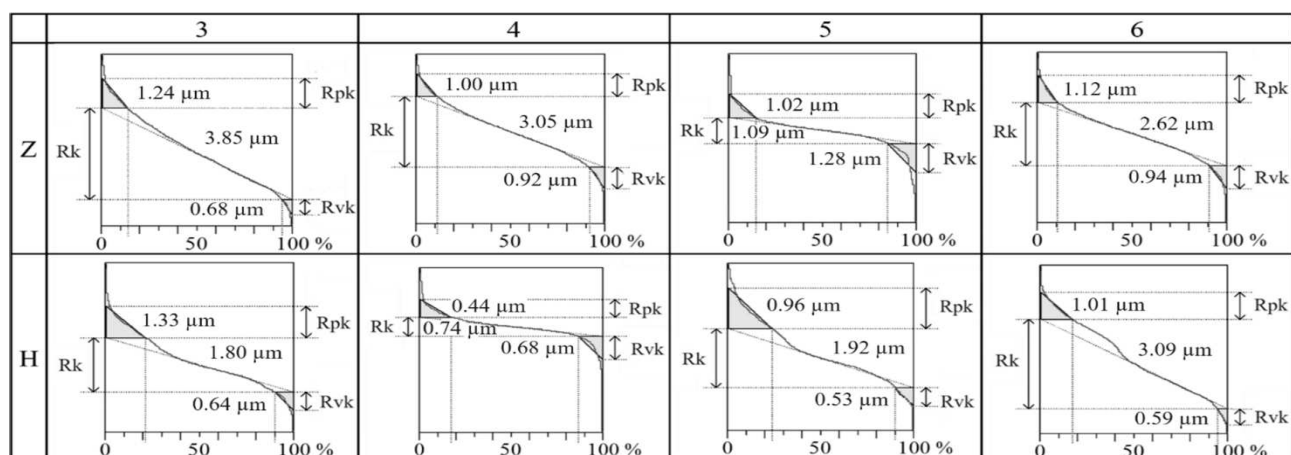


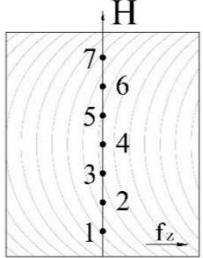
**Fig. 7** Evaluated Abbott-Firestone curves and functional parameter values of profiles measured in planes  $\underline{Z}$  and  $\underline{H}$

The change in values of the  $Rpk$  and  $Rvk$  indices is not consistent with this “geometrical effect”; their distribution is significantly influenced by another – yet unknown – effect. For this, it is advisable to analyze the Abbott-Firestone curves (AFCs) of the profiles (Fig. 7). As a result of the flattening of the roughness profile curve (measured near the tangential position in a plane), the slope of the AFCs increases, which affects the value of  $Rk$  significantly, but barely affects the values of the other two parameters. The value of

$Rpk$  in the  $\underline{E}$  and  $\underline{Z}$  planes is minimal at point 2, otherwise it is randomly distributed. In plane  $\underline{H}$  it is the lowest at the tangentially positioned point 4, and significantly higher elsewhere. The distribution of  $Rpk$  values in the  $\underline{Z}$  plane is the same as that of the  $Rku$  parameter, while in the  $\underline{E}$  and  $\underline{H}$  planes it is random. We currently do not know the reason for the diversity of the distributions; further investigations are needed to reveal this.

**Tab. 7** Roughness values in plane  $\underline{H} - 90^\circ$

Point no.	1	2	3	4	5	6	7	$\bar{R}$	$\Delta R$	$\Delta R/\bar{R}$
$Ra$ [ $\mu\text{m}$ ]	1.28	1.17	0.74	0.29	0.67	1.07	1.18	0.91	0.99	107.8%
$Rz$ [ $\mu\text{m}$ ]	6.99	6.19	5.15	2.32	4.49	5.58	7.10	5.40	4.78	88.4%
$Rsk$ [-]	0.26	0.30	0.57	-0.70	0.41	0.24	0.20	0.18	1.27	
$Rku$ [-]	2.18	2.07	3.04	4.29	2.95	2.01	2.31	2.69	2.28	84.7%
$Rpk$ [ $\mu\text{m}$ ]	1.15	1.31	1.33	0.44	0.96	1.01	1.04	1.03	0.89	86.2%
$Rk$ [ $\mu\text{m}$ ]	4.16	3.16	1.80	0.74	1.92	3.09	4.10	2.71	3.42	126.1%
$Rvk$ [ $\mu\text{m}$ ]	0.78	0.71	0.64	0.68	0.53	0.59	0.67	0.66	0.26	39.1%



Plane  $\underline{H}$  is perpendicular to the feed direction (repetition of the cycloid cutting marks), therefore the profiles recorded in the plane are nearly symmetric with its counterpart to the symmetry plane, and the roughness values of these point couples are almost identical. Based on this, we analyze the differences between the values of the symmetrical measurement point pairs on the real surface (Table 8). The value in the table is positive if the higher value was measured

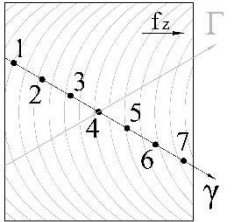
in point 1, 2 or 3. Mostly the values at points 1–3 are higher at the measurement location and the deviations are minimal (below 10%). Therefore, the profile height is minimally higher on this part of the surface, and there is a small deterioration in the wear characteristics, but improvement of the oil retention property is expected. The reason for the differences is probably the movement conditions and other variable, transient phenomena in the cutting process.

**Tab. 8** Deviations of values measured in plane  $\underline{H}$  at points symmetric to the middle plane (1–7, 2–6, 3–5)

Points:	1–7	2–6	3–5
$\Delta Ra$ [ $\mu\text{m}$ ]	0.10	0.10	0.06
$\Delta Rz$ [ $\mu\text{m}$ ]	-0.10	0.61	0.66
$\Delta Rsk$ [-]	0.06	0.06	0.15
$\Delta Rku$ [-]	-0.12	0.06	0.09
$\Delta Rpk$ [ $\mu\text{m}$ ]	0.12	0.30	0.37
$\Delta Rk$ [ $\mu\text{m}$ ]	0.06	0.08	-0.12
$\Delta Rvk$ [ $\mu\text{m}$ ]	0.12	0.12	0.11

**Tab. 9** Roughness values in plane  $\underline{\gamma} - 30^\circ$

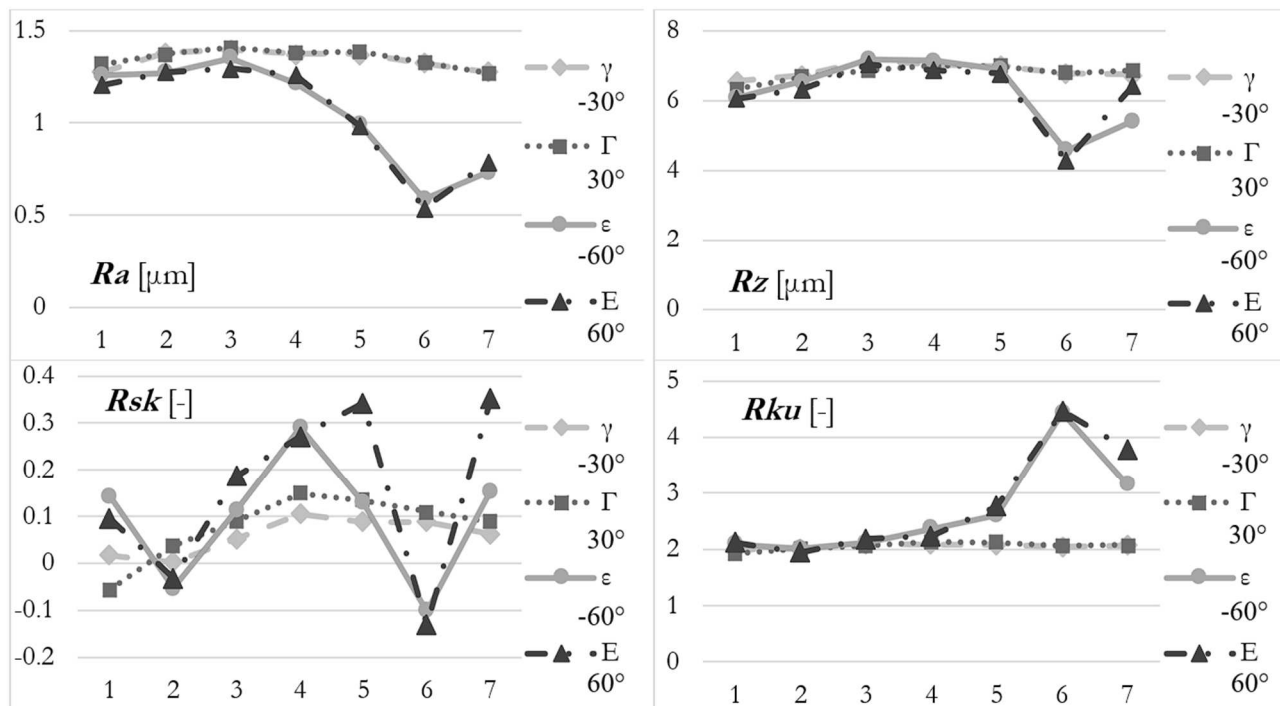
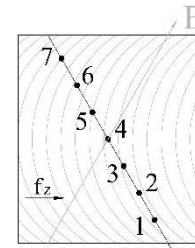
Point no.	1	2	3	4	5	6	7	$\bar{R}$	$\Delta R$	$\Delta R/\bar{R}$
$Ra$ [ $\mu\text{m}$ ]	1.28	1.38	1.40	1.37	1.37	1.32	1.27	1.34	0.12	9.3%
$Rz$ [ $\mu\text{m}$ ]	6.54	6.72	7.14	7.02	6.97	6.77	6.74	6.84	0.60	8.8%
$Rsk$ [-]	0.02	0.00	0.05	0.10	0.09	0.09	0.06	0.06	0.10	
$Rku$ [-]	1.99	2.02	2.11	2.08	2.08	2.04	2.05	2.05	0.11	5.5%
$Rpk$ [ $\mu\text{m}$ ]	0.61	0.96	1.07	0.87	0.91	0.76	0.88	0.87	0.46	52.8%
$Rk$ [ $\mu\text{m}$ ]	4.77	4.83	4.90	5.10	5.01	4.95	4.78	4.91	0.33	6.6%
$Rvk$ [ $\mu\text{m}$ ]	0.47	0.58	0.61	0.60	0.61	0.63	0.61	0.59	0.17	28.7%





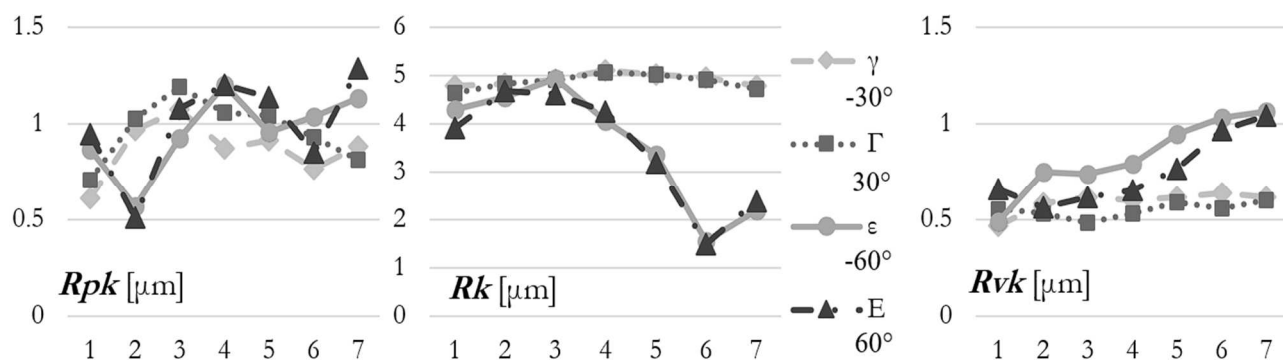
**Tab. 10** Roughness values in plane  $\varepsilon - 60^\circ$ 

Point no.	1	2	3	4	5	6	7	$\bar{R}$	$\Delta R$	$\Delta R/\bar{R}$
$Ra [\mu m]$	1.26	1.27	1.35	1.22	0.99	0.59	0.74	1.06	0.76	72.0%
$Rz [\mu m]$	6.07	6.55	7.18	7.13	6.89	4.57	5.40	6.25	2.62	41.9%
$Rsk [-]$	0.14	-0.05	0.11	0.29	0.13	-0.10	0.15	0.10	0.39	
$Rku [-]$	2.09	2.02	2.12	2.37	2.61	4.43	3.15	2.68	2.42	90.0%
$Rpk [\mu m]$	0.86	0.57	0.92	1.20	0.95	1.03	1.13	0.95	0.63	66.4%
$Rk [\mu m]$	4.29	4.55	4.93	4.05	3.35	1.54	2.18	3.56	3.39	95.3%
$Rvk [\mu m]$	0.49	0.75	0.74	0.79	0.95	1.03	1.06	0.83	0.57	69.1%

**Fig. 8** Amplitude parameter values in planes  $\gamma$  and  $\Gamma$ ,  $\varepsilon$  and  $E$  as a function of the measurement points

As the planes  $\gamma$  and  $\varepsilon$  are mirrored to planes  $\Gamma$  and  $E$  on the symmetry plane (Tables 9–10), this gives the possibility to analyze the roughness and functional characteristics of the surface if the assumed sliding direction during operation is at an angle taken in the opposite direction from the feed. For this we compare the roughness values measured in pairs of planes. For the analysis, we plot the parameter values measured in these planes (Figs. 8–9). In the symmetrical

measurement point pairs, the values are mostly similar; although there are small differences in the case of  $Rsk$ ,  $Rpk$  and  $Rvk$  parameters, the maximum deviations are  $\Delta Rsk = 0.21$ ,  $\Delta Rpk = 0.19 \mu m$  and  $\Delta Rvk = 0.18 \mu m$ . The distribution of values in the plane pairs is the same. Based on these, it can be assumed that the functional properties of the surface are almost identical along the movement directions at the same angle in both directions.

**Fig. 9** Functional parameter values in planes  $\gamma$  and  $\Gamma$ ,  $\varepsilon$  and  $E$  as a function of the measurement points

### 3.2 Analysis of roughness parameter values

In the following, we describe our findings regarding the value changes of the investigated parameters depending on the rotation of the measurement planes (direction).

For  $R_a$ ,  $R_z$  and  $R_k$  parameters, by increasing the angle of the measuring plane (sliding direction) with the feed direction from  $0^\circ$  to  $90^\circ$ , the average values decrease (by a maximum of 47%), the degree of

deviations increases from the negligible level up to 126.2%. The parameters show the same change in value in each plane, and their distribution closely follows the characteristics of the intersection of the measurement plane and the milling marks (the values decrease as the intersection angle decreases). In most cases, the percentage degree of the deviations in each plane is the largest for the  $R_k$  parameter, while the values of  $R_a$ , then  $R_z$  show smaller proportions (Tables 1–7).

**Tab. 11** Value of  $R_z/R_a$  ratio at points in the planes [ $\mu\text{m}/\mu\text{m}$ ]

Point	1	2	3	4	5	6	7	Min	Max
$\underline{\epsilon} - 60^\circ$	4.8	5.2	5.3	5.9	6.9	7.8	7.3	4.8	7.8
$\underline{\psi} - 30^\circ$	5.1	4.9	5.1	5.1	5.1	5.1	5.3	4.9	5.3
$\underline{\Delta} - 0^\circ$	4.9	4.8	4.9	4.8	4.9	4.9	4.8	4.8	4.9
$\underline{B} - 15^\circ$	4.8	4.8	4.9	4.9	4.9	5.0	4.8	4.8	5.0
$\underline{\Gamma} - 30^\circ$	4.8	4.9	4.9	5.1	5.0	5.1	5.4	4.8	5.4
$\underline{\Delta} - 45^\circ$	4.9	4.7	5.0	5.1	5.4	6.5	7.8	4.7	7.8
$\underline{E} - 60^\circ$	5.0	5.0	5.4	5.5	6.9	8.0	8.1	5.0	8.1
$\underline{Z} - 75^\circ$	5.5	5.6	5.8	6.9	8.1	7.4	6.7	5.5	8.1
$\underline{H} - 90^\circ$	5.5	5.3	7.0	7.9	6.7	5.2	6.0	5.2	7.9

Either the  $R_a$  or  $R_z$  parameter value is most often specified for surfaces on part drawings, but usually not both. The correlation between the two parameters is examined in publications. This is often expressed by the ratio  $R_z/R_a$  with value ranges typical for each machining process [32]. Its value shows the nature of the roughness profiles; the size of the areas between the curves and the center line compared to their

height. The ratios calculated in measurement planes and points are gathered in Table 11 and illustrated in Fig. 10. We find that  $R_z/R_a \approx 4.8\text{--}5.5$  is typical for the feed direction or at an angle of up to  $30^\circ$ , with minimal deviation. In the other examined planes, the ratio varies greatly between 4.7 and 8.1; the significant differences can be seen at the measurement points at which  $R_a$  and  $R_z$  values also deviate greatly.

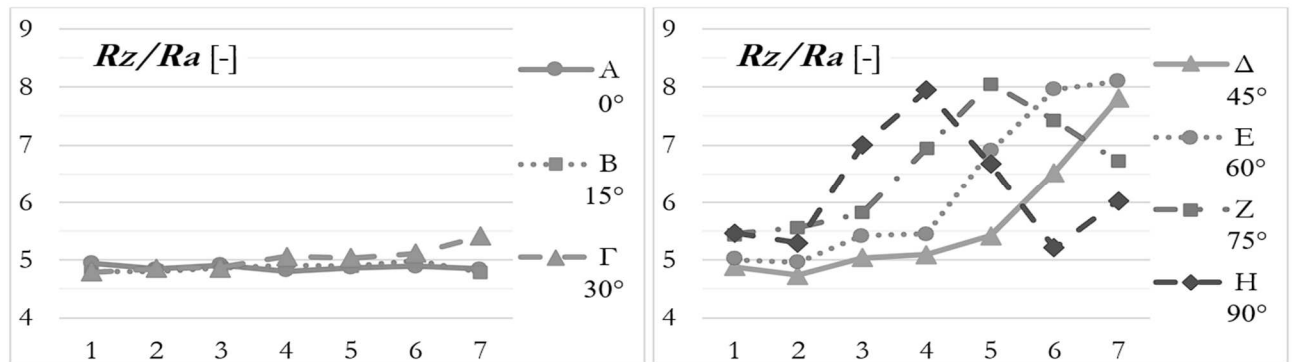


**Fig. 10**  $R_z/R_a$  ratio in the different measurement planes, depending on the measurement points

The average values of the  $R_k$  parameter in the measurement planes are almost the same and always positive, and the magnitude of the deviations increases with a greater angle of the plane (measurement direction) from the feed. Although the distribution of its values mostly differs from the case of  $R_a$  or  $R_z$ , at the point where the values of these mentioned parameters change significantly,  $R_k$  also shows significant differences. The nature of the change in values in the planes with an angle of  $0^\circ\text{--}30^\circ$  is the same as the distribution of  $R_a$  and  $R_z$  parameter values, and in plane  $\underline{\Delta}$  ( $45^\circ$ ) it is completely different. In planes  $\underline{E}\text{--}\underline{H}$  with an angle of  $60^\circ\text{--}90^\circ$ , the point

where  $R_k$  is minimal, the values of  $R_a$  and  $R_z$  are also the lowest, otherwise the distribution is different (in these planes).

The means and deviations of  $R_{ku}$  values of the profiles are the same in the two groups of planes. On the one hand, in planes  $\underline{\Delta}\text{--}\underline{\Gamma}$  with an angle of  $0^\circ\text{--}30^\circ$ , the average values are almost the same ( $\approx 2.1$ ), their deviations are minimal (below 10.2%), and their distribution is the same as described for  $R_a$ . On the other hand, in planes  $\underline{\Delta}\text{--}\underline{H}$  with an angle of  $45^\circ\text{--}90^\circ$ , the average values are similar (2.4–2.9), their differences are significant and of a similar magnitude (84%–97%), and their distribution is opposite to that

for  $Ra$  or  $Rz$ . The characteristics of the intersection of the measurement plane and the edge traces, the “geometric effect”, is well followed by the distribution of  $Rku$  values.

The values of the  $Rpk$  and  $Rvk$  parameters show different deviations and distributions than the other examined parameters. The average value of the  $Rpk$  parameter in planes  $\underline{A}$ – $\underline{H}$  is similar – it decreases to max. 38% with the increase of the measurement direction angle to  $45^\circ$ , and by further rotating the measurement plane (between  $60^\circ$ – $90^\circ$ , in planes  $\underline{E}$ – $\underline{H}$ ) the mean values are almost identical. The deviation of the values is small only in plane  $\underline{A}$ , but is significant in other directions, the change in the degree of differences becomes random as the direction angle increases. The mean value of the  $Rvk$  index increases up to 87%, in plane  $\underline{H}$  ( $90^\circ$ ) it is the same as calculated in plane  $\underline{A}$ . The deviation of the values is small in planes  $\underline{A}$ – $\underline{F}$  significant in other planes, and its degree varies randomly with increasing direction angle. The distribution of the  $Rvk$  values follows a different pattern than that described for the other indices. The reason for this may be that even a small change in the

shape of the Abbott-Firestone curves significantly affects the determination of the parameter values during the evaluation of the curve.

We rank the planes (measurement directions) according to the degree of deviation of values for the examined parameters, where the larger number means the greater change (Table 12). Since the value differences in pairs of symmetric planes ( $\underline{A}$ – $\underline{F}$  and  $\underline{E}$ – $\underline{B}$ ) are negligible, only the planes with capital letters are shown in the table as representative measurement planes and directions. In the case of  $Ra$  and  $Rsk$ , the deviation steadily increases with increasing direction angle. A very similar order can be seen for  $Rz$  and  $Rk$ ; since the deviations in planes  $\underline{A}$  and  $\underline{E}$  (the 4th and 5th rank) are almost the same, the characteristics are approximately the same here as in the previous two indices. For parameters  $Rku$  and  $Rvk$ , planes  $\underline{A}$ – $\underline{F}$  with a small ( $0^\circ$ – $30^\circ$ ) angle are also at the beginning of the order, and as the rotation angle increases, the order of the planes alters. For  $Rpk$ , the increase in deviation is not related to the increase in measurement direction angle.

**Tab. 12** Ranking list (1 – lowest deviation, 9 – largest deviation)

	$Ra$	$Rz$	$Rsk$	$Rku$	$Rpk$	$Rk$	$Rvk$
$\underline{A}$ – $0^\circ$	1	1	1	1	1	1	1
$\underline{B}$ – $15^\circ$	2	2	2	2	3	2	3
$\underline{C}$ – $30^\circ$	3	3	3	3	4	3	2
$\underline{D}$ – $45^\circ$	4	5	4	7	6	5	6
$\underline{E}$ – $60^\circ$	5	4	5	5	5	4	5
$\underline{F}$ – $75^\circ$	6	6	6	6	2	6	7
$\underline{H}$ – $90^\circ$	7	7	7	4	7	7	4

## 4 Conclusion

In the article, we examined the roughness and inhomogeneity of the topography on a face-milled surface produced with a symmetrical tool setting and single cutting marks in measurement planes perpendicular to the surface in different directions from the feed. We assumed that the characteristics of the contact during operation between the sliding surface pairs can be created by moving in the nine given different directions.

It was found that the average values of the studied amplitude and functional roughness parameters were nearly the same in the measurement directions with small ( $0^\circ$ – $30^\circ$ ) or large ( $45^\circ$ – $90^\circ$ ) angles to the feed direction, but between the two groups average parameter values were significantly different. The degree of their deviations in measurement directions different from the feed direction by  $0^\circ$ – $30^\circ$  was small (up to 10%), while in the direction with a larger angle of  $45^\circ$ – $90^\circ$  they were significant (up to 126%).

The magnitude of deviations of values and the nature of their change is primarily related to the extent

to which the angle between the measurement plane (measurement direction) and the milling marks changed. In the plane rotated from the feed direction with an angle of  $45^\circ$  or more, the minimum  $Ra$ ,  $Rz$ ,  $Rsk$ ,  $Rk$ , and maximum  $Rku$  values were at the measurement location where it was nearest to the position tangential to the milling marks. The degree of asymmetry of the surface texture (cycloid edge traces) to the symmetry plane is minimal, so the roughness values and deviations are nearly symmetric to the symmetry plane and the changing cutting conditions (the direction of movement of the tool edge due to the cutting process kinematics and the size of the chip cross-section) did not significantly affect them (the values and deviations).

The values of  $Rpk$  and  $Rvk$  parameters showed different magnitudes and changes compared to the other examined parameters. This could have been influenced by the fact that if the shape of the Abbott-Firestone curves from the measured profiles changes even slightly, it significantly affects the parameter values determined to have a large standard deviation during the evaluation of the curve.

The values of amplitude  $R_a$ ,  $R_z$ , and  $R_{sk}$  and functional  $R_k$  parameters showed a good correlation between the increase of the deviations calculated in the examined planes and the increase of the measurement direction angle, while a weak correlation was observed for  $R_{ku}$  and  $R_{vk}$  and no correlation was found for  $R_{pk}$ . Therefore, we suggest that the roughness unevenness of the face-milled surface in the different measurement directions can be well characterized by  $R_a$ ,  $R_z$ ,  $R_{sk}$ , and  $R_k$  parameters.

Based on the results of the study, if the face-milled surface slides during operation in a direction parallel to the feed or different by no more than  $30^\circ$  from the feed, its functional characteristics are almost the same (on different parts of the surface). These are higher friction, a longer running-in period, lower wear resistance, less dimensional stability and lower lubrication retention, which are typical for a face-milled surface compared to a ground surface. When moving at a greater angle than this, if the part of the surface is in contact where it is almost tangential to the edge traces, it is expected that the friction coefficient will be minimal and the wear resistance and dimensional stability will be the best compared to other parts of the topography, and the lubricant retention ability will not change significantly.

We found that it is advisable to perform the profile measurement required to check the production quality during machining with the  $R_a$  parameter [4] in the usual feed direction, if possible in the symmetry plane, where almost the same roughness value can be measured regardless of the measurement location. Profiles measured in a different direction and/or location than the symmetry plane can give significantly different roughness values [33]. While the  $R_z/R_a$  ratio of profiles measured in the feed direction, or in a direction different from it by up to  $30^\circ$  is similar (approx. 4.8–5.5), the ratio in the further rotated planes (at  $45^\circ$ – $90^\circ$  angle) also differs greatly.

## References

- [1] STOUT, K., BLUNT, L. (2000). *Three dimensional surface topography*. Penton Press, London. ISBN: 978-1-8571-8026-7
- [2] GUO, S., ZHANG, J., JIANG, Q., ZHANG, B. (2022). Surface integrity in high-speed grinding of Al6061T6 alloy. In: *CIRP Annals*, Vol. 71, No. 1, pp. 281 – 284. ISSN: 0007-8506
- [3] HORVÁTH, R., CZIFRA, Á., DRÉGELYI-KISS, Á. (2015). Effect of conventional and non-conventional tool geometries to skewness and kurtosis of surface roughness in case of fine turning of aluminium alloys with diamond tools. In: *The International Journal of Advanced Manufacturing Technology*, Vol. 78, pp. 297 – 304. ISSN: 0268-3768
- [4] GADELMAWLA, E., KOURA, M., MAKSOUD, T., ELEWA, I., SOLIMAN, H. (2002). Roughness parameters. In: *Journal of Materials Processing Technology*, Vol. 123, No. 1, pp. 133 – 145. ISSN: 0924-0136
- [5] SEDLACEK, M., PODGORNIK, B., VIZINTIN, J. (2012). Correlation between standard roughness parameters skewness and kurtosis and tribological behaviour of contact surfaces. In: *Tribology International*, Vol. 48, pp. 102 – 112. ISSN: 0301-679X
- [6] WOJCIECHOWSKI, Ł., GAPINSKI, B., FIRLIK, B., MATHIA, T. (2020). Characteristics of tram wheel wear: Focus on mechanism identification and surface topography. In: *Tribology International*, Vol. 150, ArtNo. 106365. ISSN: 0301-679X
- [7] PAWLUS, P., REIZER, R., ZELASKO W. (2020). Prediction of Parameters of Equivalent Sum Rough Surfaces. In: *Materials*, Vol. 13, ArtNo. 4898. MDPI. Basel, Switzerland. ISSN: 1996-1944
- [8] WOJCIECHOWSKI Ł., GAPIŃSKI, B., PACZKOWSKA, M., MATHIA, T. (2022). Investigations of the complex wear mechanisms of tram wheel tyres. In: *Wear*, Vol. 500, ArtNo. 204354. ISSN: 0043-1648
- [9] GRZESIK, W., ZAK, K. (2012). Modification of surface finish produced by hard turning using superfinishing and burnishing operations. In: *Journal of Materials Processing Technology*, Vol. 212, pp. 315 – 322. ISSN: 0924-0136
- [10] TODHUNTER, L., LEACH, R., LAWES, S., BLATEYRON, F. (2017). Industrial survey of ISO surface texture parameters. In: *CIRP Journal of Manufacturing Science and Technology*, Vol. 19, pp. 84 – 92. ISSN: 1755-5817
- [11] LEACH, R. (2001). The Measurement of Surface Texture using Stylus Instruments. In: *Measurement Good Practice Guide*, No. 37, pp. 1-85. Crown Copyright, Teedington. ISSN: 1368-6550.
- [12] SAHAY, C., GHOSH, S. (2018). Understanding surface quality: beyond average roughness ( $R_a$ ). In: *2018 ASEE Annual Conference & Exposition*, ArtNo. 31176. ASEE American Society for Engineering Education, Salt Lake City, Utah

- [13] WHITEHOUSE, D. (2011). *Handbook of Surface and Nanometrology*. CRC Press, Boca Raton. ISBN: 978-1-4200-8201-2
- [14] PAWLUS, P., REIZER, R., WIECZOROWSKI, M. (2020). Characterization of the shape of height distribution of two-process profile. In: *Measurement*, Vol. 153, ArtNo. 107387. ISSN: 0263-2241
- [15] YAN, X., WANG, X., ZHANG, Y. (2014). Influence of roughness parameters skewness and kurtosis on fatigue life under mixed elastohydrodynamic lubrication point contacts. In: *Journal of Tribology*, Vol. 136, No. 3, ArtNo. 031503. ISSN: 0742-4787
- [16] EGEA, A.J.S., MARTYNENKO, V., SIMONCELLI, A., SERRANCOLI, G., KRAHMER D.M. (2022). Sliding abrasive wear when combining WEDM conditions and polishing treatment on H13 disks over 1045 carbon steel pins. In: *The International Journal of Advanced Manufacturing Technology*, Vol. 118, pp. 183 – 193. ISSN: 0268-3768
- [17] ZAGÓRSKI, I., KORPYSA, J. (2019). Surface Quality in Milling of AZ91D Magnesium Alloy. In: *Advances in Science and Technology. Research Journal*, Vol. 13, No. 2, pp. 119 – 129. Lublin University of Technology, Polish Society of Ecological Engineering. Lublin, Poland. ISSN: 2299-8624
- [18] PAWLUS, P., REIZER, R., WIECZOROWSKI, M. (2021). Analysis of surface texture of plateau-honed cylinder liner – A review. In: *Precision Engineering*, Vol. 72, pp. 807 – 822. ISSN: 0141-6359
- [19] ZHANG, Y., BAI, Q., WANG, P. (2023). 3D surface topography analysis and functionality-related performance of the machined surface in slot micro-milling titanium alloy Ti6Al4V. In: *The International Journal of Advanced Manufacturing Technology*, Vol. 127, pp. 1609 – 1629. ISSN: 0268-3768
- [20] SINHA, M.K., KISHORE, K., SHARMA, P. (2023). Surface integrity evaluation in ecological nanofluids assisted grinding of Inconel 718 superalloy. In: *Proceedings of the Institution of Mechanical Engineers, Part E: Journal of Process Mechanical Engineering* (Pre-published, Digital release, DOI: 10.1177/09544089231171042) ISSN: 2041-3009
- [21] GRZESIK, W. (2016). Prediction of the Functional Performance of Machined Components Based on Surface Topography: State of the Art. In: *Journal of Materials Engineering and Performance*, Vol. 25, pp. 4460 – 4468. ISSN: 1059-9495
- [22] HAMDI, A., MERGHACHE, S.M. (2021). Impact of Abrasive Grit Size and MQL Supply on the Surface Roughness in Belt Grinding of a Case Hardened Steel. In: *Jordan Journal of Mechanical and Industrial Engineering*, Vol. 15, No. 5, pp. 441 – 449. ISSN: 1995-6665
- [23] BENKHELIFA, O., CHERFIA, A., NOUIOUA, M. (2022). Modeling and multi-response optimization of cutting parameters in turning of AISI 316L using RSM and desirability function approach. In: *The International Journal of Advanced Manufacturing Technology*, Vol. 122, pp. 1987 – 2002. ISSN: 0268-3768
- [24] DAS, J., LINKE, B. (2017). Evaluation and systematic selection of significant multi-scale surface roughness parameters (SRPs) as process monitoring index. In: *Journal of Materials Processing Technology*, Vol. 244, pp. 157 – 165. ISSN: 0924-0136
- [25] KORZENIEWSKI, D., ZNOJKIEWICZ, N. (2021). Surface texture of the milled surface of aluminum-ceramic composite. In: *Journal of Mechanical Science and Technology*, Vol. 35, pp. 2879 – 2884. ISSN: 1738-494X
- [26] SZTANKOVICS, I. (2023). Preliminary Study on the Function-Defining 3D Surface Roughness Parameters in Tangential Turning. In: *International Journal of Integrated Engineering*, Vol. 15, No. 7, pp. 72 – 81. ISSN: 2229-838X
- [27] HAMDI, A., MERGHACHE, S.M., ALIOUANE, T. (2020). Effect of cutting variables on bearing area curve parameters (BAC-P) during hard turning process. In: *Archive of Mechanical Engineering*, Vol. 67, No. 1, pp. 73 – 95. ISSN: 0004-0738
- [28] ZAGÓRSKI, I., KORPYSA, J. (2020). Surface quality assessment after milling AZ91D magnesium alloy using PCD tool. In: *Materials*, Vol. 13, No. 3, ArtNo. 617. MDPI. Basel, Switzerland. ISSN: 1996-1944
- [29] ZALESKI, K., SKOCZYLAS, A., BRZOZOWSKA, M. (2017). The effect of the conditions of shot peening the Inconel 718 nickel alloy on the geometrical structure of the surface. In: *Advances in Science and Technology. Research Journal*, Vol. 11, No. 2, pp. 205 – 211. Lublin University of Technology, Polish Society of Ecological Engineering. Lublin, Poland. ISSN: 2299-8624

- [30] SMITH, G.T. (2008). *Cutting Tool Technology: Industrial Handbook*. Springer-Verlag, London. ISBN: 978-1-8480-0204-3
- [31] BITELLI, G., SIMONE, A., GIRARDI, F., LANTIERI, C. (2012). Laser Scanning on Road Pavements: A New Approach for Characterizing Surface Texture. In: *Sensors*, Vol. 12, No. 7, pp. 9110 – 9128. MDPI. Basel, Switzerland. ISSN: 1424-8220
- [32] PALÁSTI, K., SIPOS, S., CZIFRA, Á. (2012). Interpretation of “ $R_z = 4 \times R_a$ ” and other roughness parameters in the evaluation of machined surfaces. In: *Proceedings of the 13th International Conference on Tools: ICT 2012*, pp. 237 – 244. University of Miskolc, Miskolc, Hungary. ISBN: 978-963-9988-35-4
- [33] NAGY, A., KUNDRÁK, J. (2022). Analysis of inhomogeneity of surfaces milled with symmetrical, down-milling, and up-milling settings. In: *Development in Machining Technology: Scientific – Research Reports vol.10*, pp. 51 – 62. Cracow University of Technology, Cracow. ISBN: 978-80-553-4133-0